

Chapter 2

Controlled power operation of 12-pulse converter

2.1 Introduction

Many large industrial loads such as used in Steel Plants, Mining etc. need converters (MW rating) feeding DC motor drives controlling to and fro motion of the mechanical load. Under such drive environment there are wide fluctuations in the Var demand by the converter. Those apart, frequent harmonic related problems are also encountered. Passive filters have been considered good for harmonic current and displacement power factor compensation. They also are capable of drawing fixed lead Var at fundamental frequency. When there is a variation of the Var demand by the non-linear loads connected at point of common coupling (PCC), as in the case of a phase controlled converter feeding DC motor drive, the passive filters may either over compensate or under compensate reactive power. Thus the power system continues to be affected by the fluctuations in Var demand of the load[3].

In the past, many researchers have suggested various Var control techniques using multiple passive filters, while operating with thyristorized non-linear loads. One such method is the use of Thyristor switched filter (TSF). By switching on or off the TSF, the compensator can dynamically adjust reactive power compensation according to the Var demands of the phase controlled rectifier system.

Among several other methods for converter power factor improvement is asymmetrical firing control for a 12-pulse converter system where in two 6-pulse converters operate in cascade. In reduced Var operation mode, each 6-pulse converter is fired symmetrically. But the two converters are controlled as asymmetrical groups. Superconducting magnetic energy storage systems are getting increasing interest in applications of power flow stabilization and control in the transmission network level. This trend is mainly supported by the rising integration of large scale wind energy power plants into the high-power utility system and by major features of SMES units. Due to arbitrary variations of wind speed, Load fluctuation is occurred. So minimization of fluctuation is essential for power system security. 12 pulse converter has the certain freedom in choosing active & Reactive power. By utilizing the reactive power modulation capacity of the converter, the inductor-converter unit of function as a static VAR controller using a switched capacitor bank, while acting as a load frequency stabilizer at the same time. The converter is a voltage source converter with a controller.

2.2 Operation of 12-pulse converter

The 12- pulse converter is constructed using two 6- pulse converter connected in series and phase shifted by 30 degree through star / star and star / delta transformers. As shown in Figure 2.1. The two three-phase star-delta and star-star transformer sources set the supply for 6-pulse bridges phase displaced by 30 degrees.

This configuration is useful for applications where converter load rating, which are mostly DC drives, range beyond MW rating[4]. When these drives are operated at very low speeds the VAR drawn tend to be extremely large due to high motor current being drawn to maintain high operating torque. With 12-pulse converters it is also possible to achieve low var (Q) by operating in asymmetrical firing mode.

2.3 Active and reactive power of a 12-pulse converter

The active and reactive power required by the converter is the total power required by two 6- pulse converter and its depends on the individual firing angles. The P vs Q locus

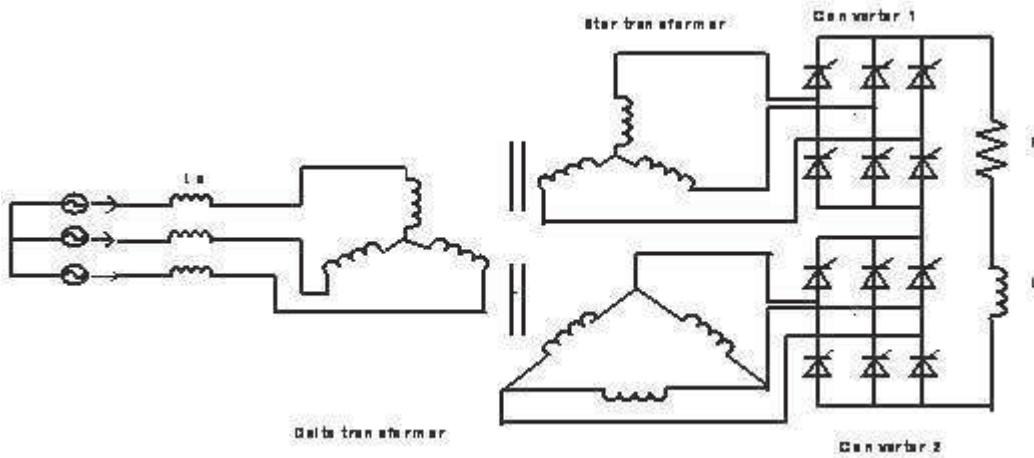


Figure 2.1: 12 pulse converter

of each 6-pulse converter bridge traces a semicircle with radius of V_{d0} and I_d where V_{d0} is the maximum dc voltage and I_d is load current as shown in Figure 2.2. Depending on the positioning of the point on the semicircular loci of the two converter bridges, there can be a number of operating modes in a 12-pulse thyristor bridge.

The power locus of a 12-pulse converter can be obtained based on the theory of converter operation according to which, the voltage due to each constituent 6-pulse converter in the absence of source inductance is given by,

$$V_{d_i} = V_{d_0} \cos \alpha_i = \frac{3V_{max}}{\pi} * \cos \alpha_i \quad (2.1)$$

where,

V_{max} = peak line-line voltage of the input supply.

α_i = Converter firing angle

The subscript i identifies the 6-pulse converter number 1 or 2. Multiplying the DC load current I_d on both sides we get,

$$P_{d_i} = V_{d_i} * I_d = V_{d_0} * I_d \cos \alpha_i \quad (2.2)$$

Where, P_{d_i} is the active power transfer through converter i . The maximum active power transfer through the converter i occurs at $\alpha_i = 0$, which can be expressed as $V_{d_0} * I_d$

The active and reactive power loads and, presented by the 12-pulse converter are the sum of the contribution made by each converter and can be expressed as

$$P_d = P_{max} (\cos \alpha_1 + \cos \alpha_2) \quad (2.3)$$

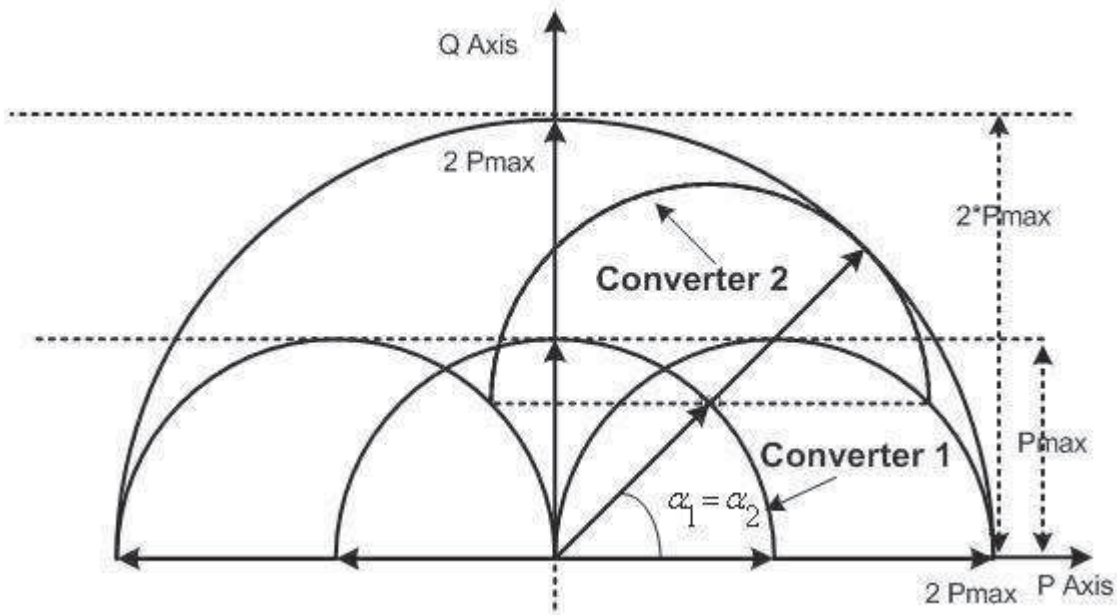


Figure 2.2: Active/Reactive Power Locus for symmetrical Firing angle operation

$$Q_d = P_{max} (\sin \alpha_1 + \sin \alpha_2) \quad (2.4)$$

Figure 2.3 shows the equal firing angle mode with the source inductance. The radius of the semi circle is depends on the current through the load.

The complete semicircular range of the $P - Q$ locus is not achievable due to the equivalent commutating reactance, which represents the commutation overlap. The commutation overlap depends mainly on the leakage reactance of the transformer connecting the converter to the system bus and source inductance. The power locus of a 12-pulse converter can be obtained based on theory of converter operation according to which, the voltage due to each constituent 6-pulse converter with considering the source inductance is

$$V_{d_i} = V_{d_o} \cos \alpha_i - X_c I_d \quad (2.5)$$

Where

V_{d_i} = DC side voltage

V_{d_o} = No load maximum dc voltage of 6-pulse converter

α_i = Converter delay angle

where subscript identifies the 6-pulse converter number 1 or 2.

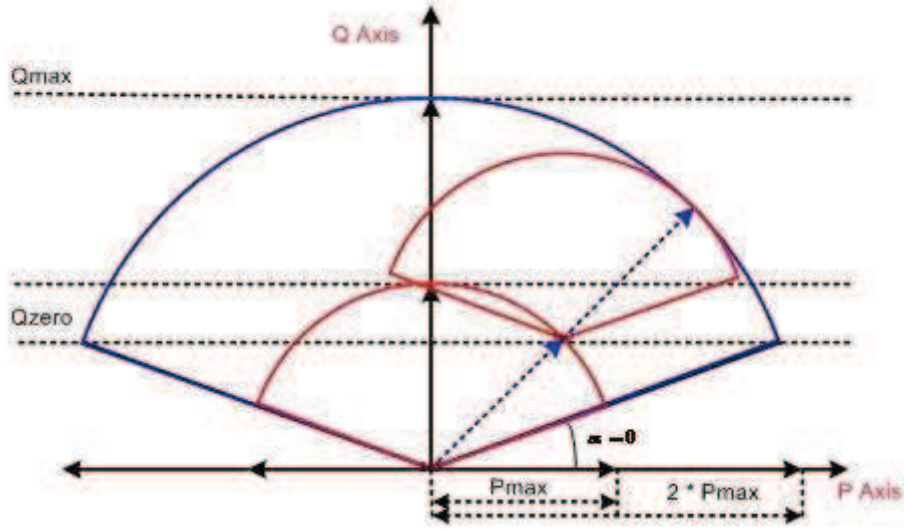


Figure 2.3: Active Power vs Reactive power

Total active power drawn by the converter is given by

$$P_d = P_{d_1} + P_{d_2} = V_{d_o} I_d (\cos \alpha_1 + \cos \alpha_2) - 2I_d^2 X_c \quad (2.6)$$

Where,

$$X_c = \frac{3\omega L_s}{\pi}$$

The power factor seen from system side is

$$\cos \phi = \frac{P_d}{S_{max}} \text{ where } S_{max} = 2V_{d_o} I_d$$

$$\cos \phi = \cos \alpha - \frac{I_d X_c}{V_{d_o}} \quad (2.7)$$

and

$$\sin \phi = (1 - \cos^2 \phi)^{\frac{1}{2}} \quad (2.8)$$

So, existence of the equivalent commutating reactance imposes a limit on the minimum power factor angle.

For each 6- pulse converter,

$$\cos \phi_i = \cos \alpha_i - \frac{I_d X_c}{V_{d_o}} \quad (2.9)$$

$$\sin \phi = (1 - \cos^2 \phi)^{\frac{1}{2}} \quad (2.10)$$

In the case of equal α mode of converter control

$$\alpha_1 = \alpha_2 = \alpha$$

$$P_d = 2V_d I_d \cos \alpha - 2I_d^2 X_c \quad (2.11)$$

At any point on the P-Q locus, for a given P_d , reactive power Q_d is expressed as $Q_d = Q_{d_1} + Q_{d_2}$ where Q_{d_1}, Q_{d_2} are the reactive power drawn by each converter

Theoretically, the converter can be operated over the full 180° range of delay angle. But because of the effect of the source inductance, its operation is limited. The commutation angle is given by

$$\mu = \cos^{-1} \left[\cos \alpha - \frac{2\omega\omega_s I_d}{\sqrt{2}V_{LL}} \right] \quad (2.12)$$

Theoretically, the converter can be operated over the full 180° range of delay angle. However, the line commutated converters have to be operated between the $\alpha + \mu$ to end-stop. The end stop is defined as the maximum firing angle that can be applied to the converter so that the converter can be operated without commutation failure, beyond these limit, risk of commutation failure. Figure 2.3 shows the variation with simultaneous variation both converter firing angles, the variation of active power and reactive power. The center is also shifting from zero as the source inductance is increased. And also the value of is also increasing. The Figure 2.4 shows the variation of overlap angle with the firing angle of the converter with different values of source inductance. As the source inductance is increased the variation range for firing angle of the converter is reduced and operating points are also reduced.

2.4 Active power with variation in firing angles

The source inductance has considerable effect of the operation of any converter. Ideally any converter has been operated for 0° to 180° firing angle. Figure 2.5 and Figure 2.6 shows composite [6] 3-Dimensional plot of the per-unit (p.u) active power against simultaneous variation of firing angles of both the converters. Here x, y, z axes represents firing angles and net pu Active power drawn by the 12-pulse converter. The net active power required by the converter is 1 p.u. at (α_1, α_2) equal to (0,0) and zero at (α_1, α_2) equal (0,180), (90,90) and (180,0) and -1 p.u. at (180,180) without source inductance. The net active power drawn with source inductance at equal to zero is less than 1. pu. Similarly at

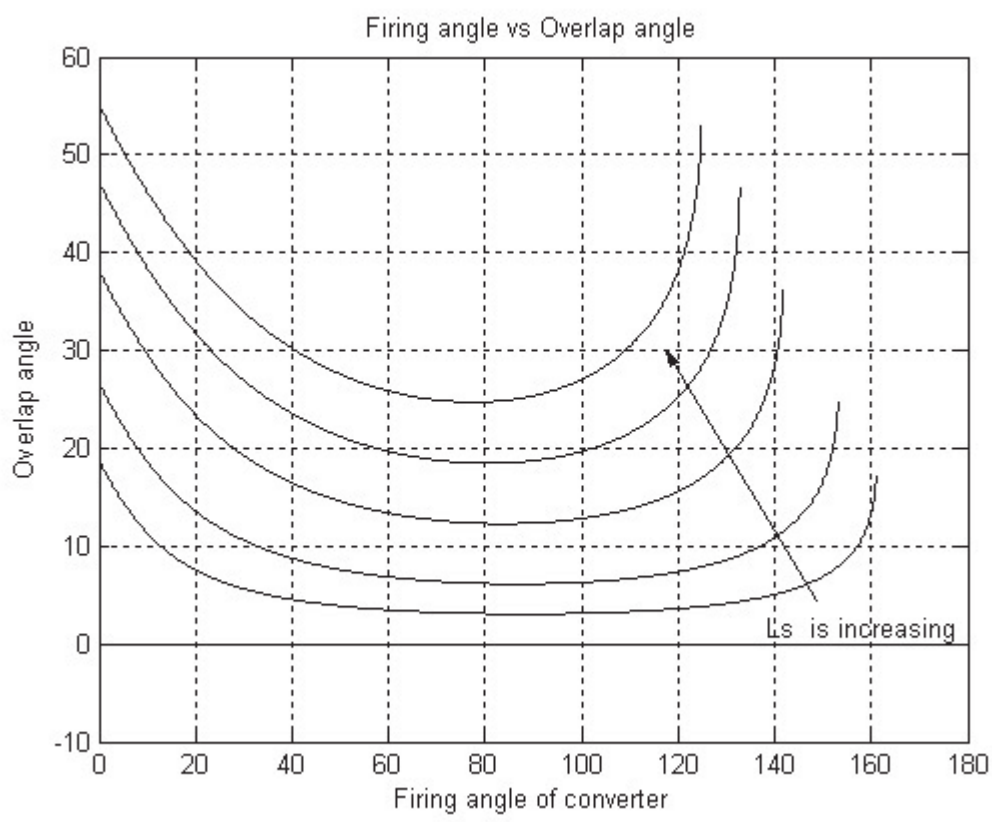


Figure 2.4: Effect of Overlap angle on Firing angle

(α_1, α_2) equal to end-stop, the net active power drawn by the converter is less than -1 p.u. As the source inductance is increased the operating region is decreased and the end stop value of the firing angle of the each converter is also reduced. The diagram also shows the projection of constant P operation of converter shown in x-y plane in Figure 2.5.

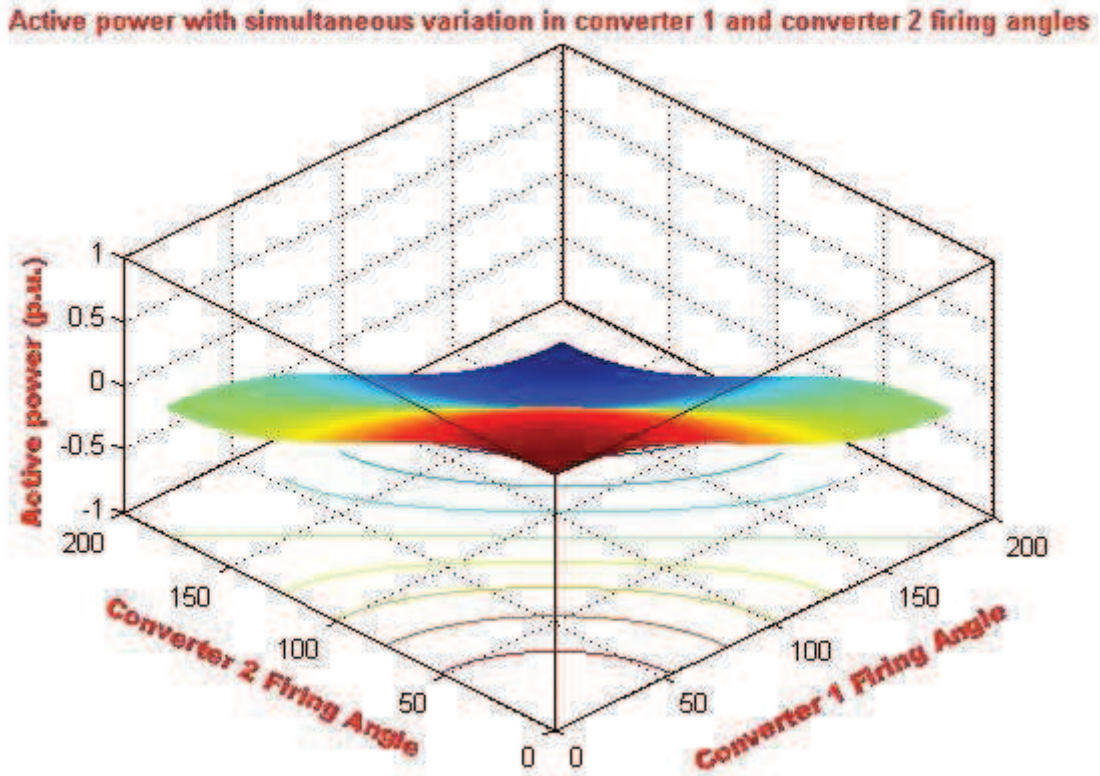


Figure 2.5: 3-D Plot of active power with simultaneous variation in converter 1 and converter 2 firing angles without source inductance

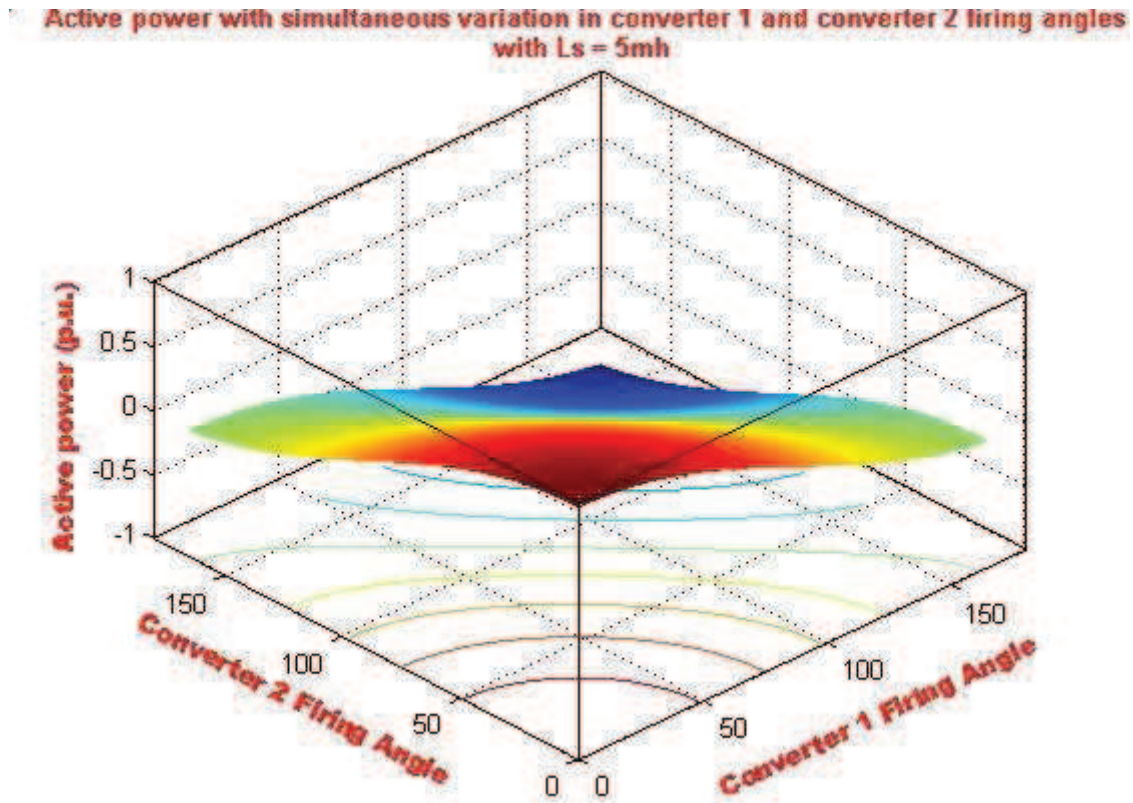


Figure 2.6: 3-D Plot of active power with simultaneous variation in converter 1 and converter 2 firing angles with source inductance

2.5 Reactive power with variation in firing angles

The source inductance has considerable effect of the operation of any converter. Ideally any converter has been operated for 0^0 to 180^0 firing angle. Figure 2.7 and Figure 2.8 shows composite 3-Dimensional plot of the per-unit (p.u) reactive power against simultaneous variation of firing angles of both the converters for with and without source impedance. The net reactive power drawn by the converter is zero at (α_1, α_2) equal to $(0, 0)$, $(0, 180)$, $(180, 0)$ and $(180, 180)$ and 1 p.u. at (α_1, α_2) equal to $(90, 90)$ without source inductance. . The net reactive power drawn with source inductance at equal to $(0, 0)$ is higher than zero. Similarly at (α_1, α_2) equal to end stop, the net reactive power drawn by the converter is higher than zero. As the source inductance is increased the operating region is decreased and the end stop value of the firing angle of the individual converter is also reduced. The diagram also shows the projection of constant Q operation of the converter,

which are concentric circles plotted on the x-y plane.

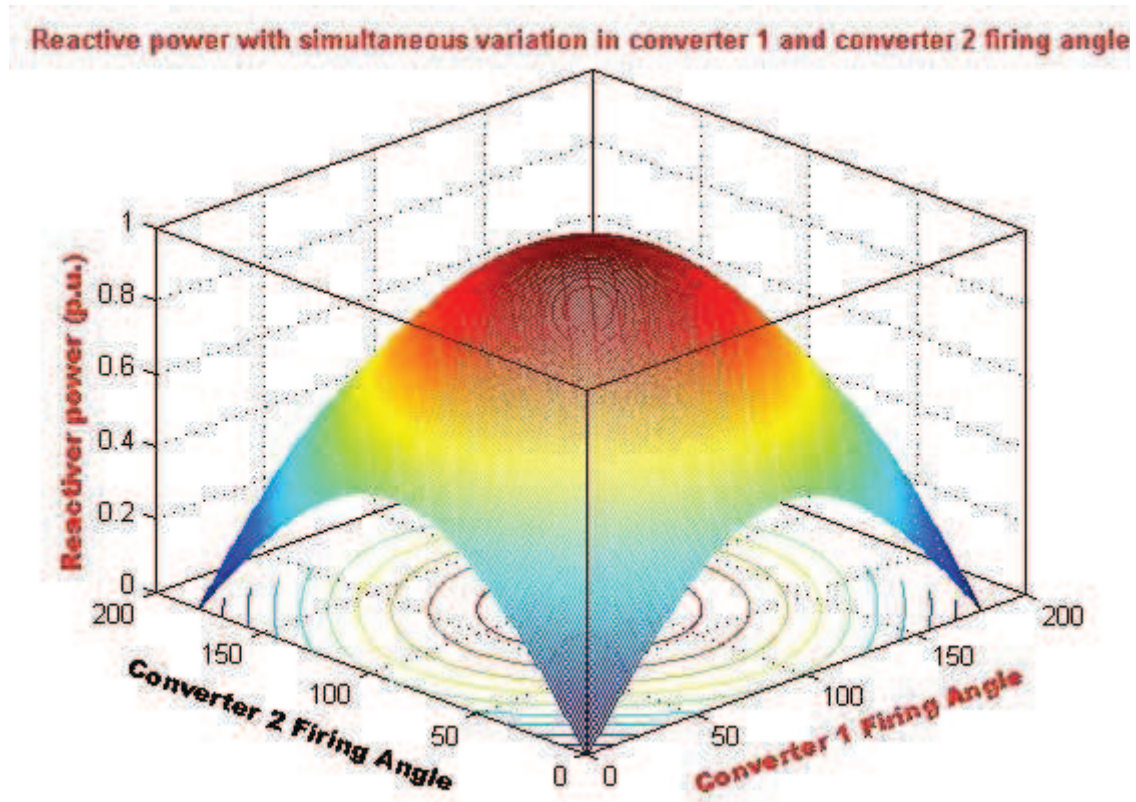


Figure 2.7: 3-D Plot of reactive power with simultaneous variation in converter 1 and converter 2 firing angles without source inductance

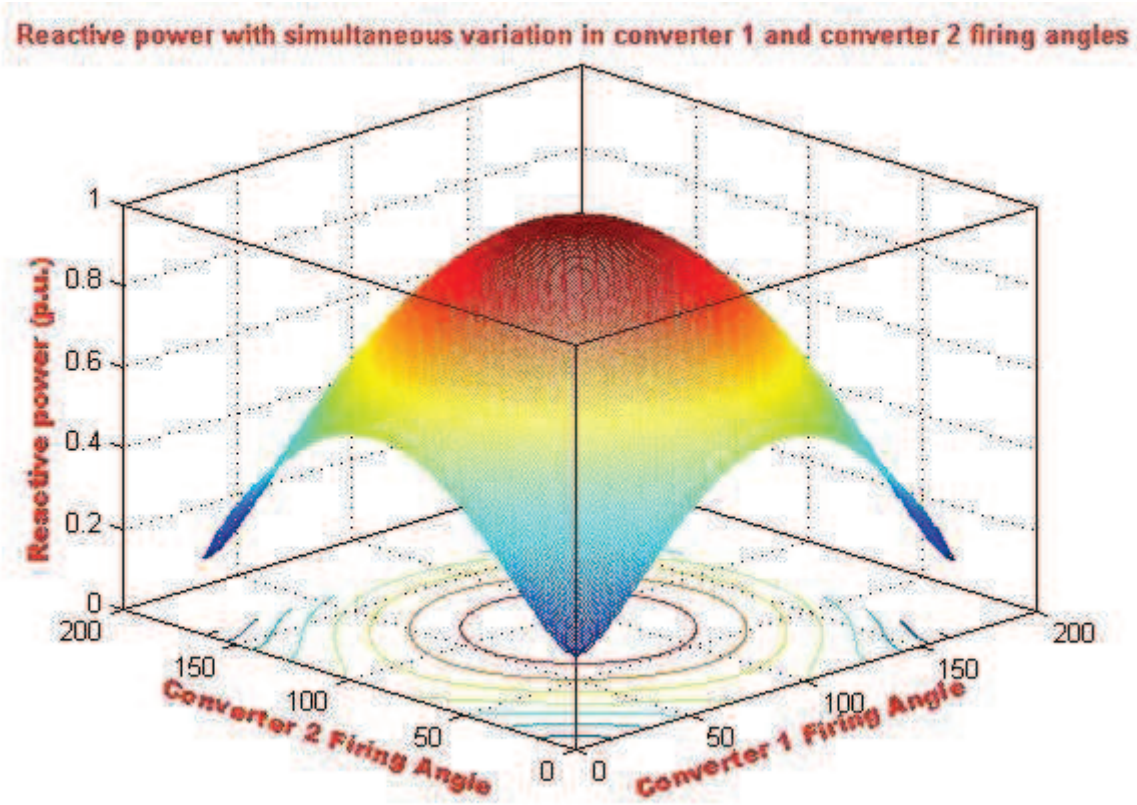


Figure 2.8: 3-D Plot of reactive power with simultaneous variation in converter 1 and converter 2 firing angles with the effect of source inductance

2.6 Constant reactive power operation

The 12-pulse rectifier operation in constant Var mode can be explained using Figure 2.2. For a constant var operation if a line parallel to x-axis be drawn at height equal to the required var, any point on the line could be achieved using combinations of different firing angles α_1 and α_2 . There are many combinations of firing angles α_1 and α_2 for achieving a required Q. It can be observed that for a constant reactive power operation of the converter, the maximum possible active power, both in rectifier and inverter mode, occur under symmetrical firing angle operation. While observing constant var operation there are possibilities for the net var drawn by the converters may lie either above or below the peak var absorption capability of one of the converters. Under certain operating conditions the desired net reactive power q_{set} can be expressed in per unit (p.u.) values

as sum of the reactive power drawn by constituent converters.

$$q_{set}(p.u.) = (\sin\phi_1 + \sin\phi_2) * 0.5 \quad (2.13)$$

At zero firing angle of the both converter the reactive power is given by,

$$q_{zero}(p.u.) = \sqrt{\frac{X_c I_d}{V_{do}}}$$

$$q_{max}(p.u.) = S_{max}$$

$$q_{mid}(p.u.) = (q_{max}(p.u.) + q_{zero}(p.u.)) * 0.5 \quad (2.14)$$

The operation of the 12-pulse converter under this mode can be categorized in two cases.

Case(a) $q_{set} \geq q_{mid}$

In this case, there is a minimum firing angle at which each of the converters must work in order to maintain a constant var. As shown in Figure 2.9, the minimum firing angle at which one converter will operate will occur when the other converter operates at firing angle $\alpha + \mu = 90$. Thus the minimum firing angle at which each of the converters should operate are given as under:

$$q_1 = \sqrt{1 - \left(\cos\alpha_1 - \frac{X_c I_d}{S_{max}} \right)^2} \quad (2.15)$$

$$q_2 = \frac{q_{set} - q_1}{\sqrt{1 - \left(\cos\alpha_2 - \frac{X_c I_d}{S_{max}} \right)^2}}$$

$$\alpha_2 = \cos^{-1} \left[\left(\sqrt{1 - q_2^2} + \frac{X_c I_d}{S_{max}} \right)^2 \right]$$

Or

$$\alpha_2 = \pi - \cos^{-1} \left[\left(\sqrt{1 - q_2^2} + \frac{X_c I_d}{S_{max}} \right)^2 \right] \quad (2.16)$$

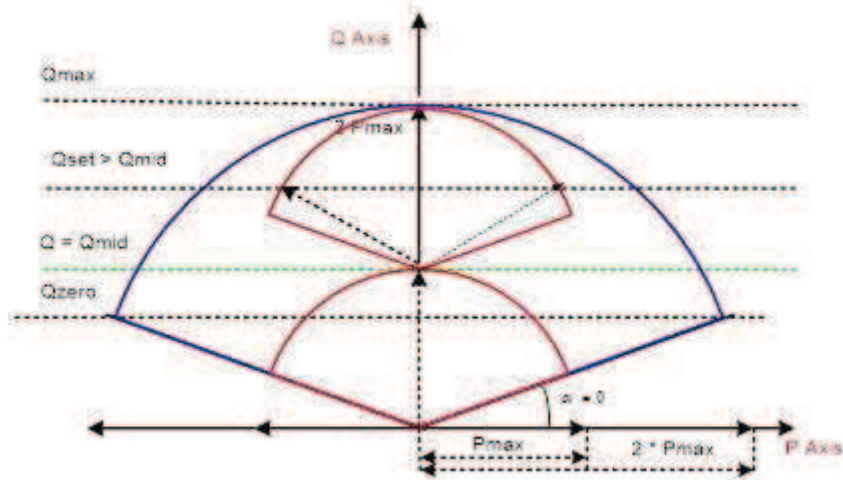


Figure 2.9: Limiting firing angles of operation of 12- pulse converter at $q_{set} \geq q_{mid}$

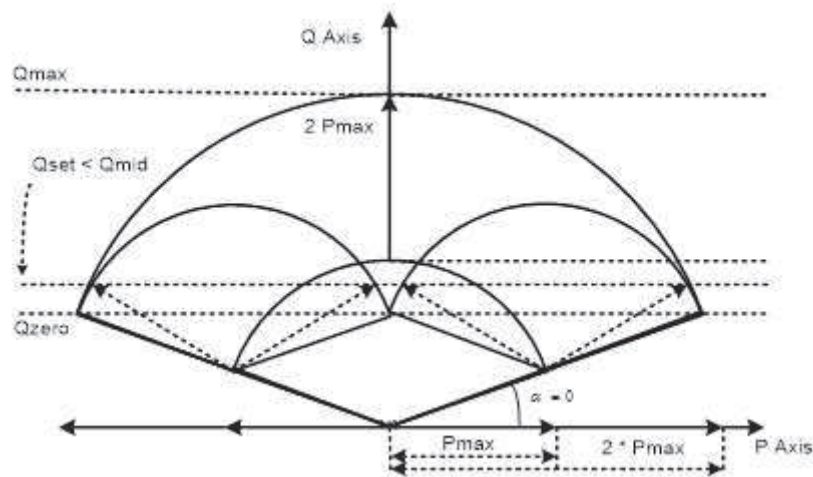


Figure 2.10: Limiting firing angles of operation of 12- pulse converter at $q_{set} \leq q_{mid}$

Case(b) $q_{set} \leq q_{mid}$

In this case when the converter is operating in first quadrant, there is a maximum firing angle up to which the converter can operate and satisfy the reactive power condition. The firing angle of the one converter is zero and other converter is

$$\alpha_2 = \cos^{-1} \left[\left(\sqrt{1 - q_2^2} + \frac{X_c I_d}{S_{max}} \right)^2 \right] \quad (2.17)$$

Or

$$\alpha_2 = \pi - \cos^{-1} \left[\left(\sqrt{1 - q_2^2} + \frac{X_c I_d}{S_{max}} \right)^2 \right] \quad (2.18)$$

This maximum firing angle for one converter occurs when the other converter operates at a firing angle for minimum Q (i.e. α_1). And when the 12-pulse converter is operating in the second quadrant, and when one of the constituent converters is operating at minimum Q when $\alpha_1 = \text{end stop}$, the minimum firing angle at which the converter must operate satisfying the reactive power criteria is

$$\alpha_2 = \cos^{-1} \left[\left(\sqrt{1 - q_2^2} + \frac{X_c I_d}{S_{max}} \right)^2 \right] \quad (2.19)$$

Or

$$\alpha_2 = \pi - \cos^{-1} \left[\left(\sqrt{1 - q_2^2} + \frac{X_c I_d}{S_{max}} \right)^2 \right] \quad (2.20)$$

Figure 2.11 represents the range of firing angles at which the two converters need to operate for different constant Var operating conditions. This figure depicts both the regions of operation. As the value of the source inductance is varied, the region of operation and range of is also varied. Figure 2.12 and Figure 2.13 shows the same effect for different values of source impedance. Same effect can also be observed for variation of the load current as shown in Figure 2.14 and Figure 2.15 with source impedance. Figure 2.11 represents the range of firing angles at which the two converters need to operate for different constant Var operating conditions. This figure depicts both the regions of operation. As the value of the source inductance is varied, the region of operation and range of is also varied. Figure 2.12 and Figure 2.13 shows the same effect for different values of source impedance. Same effect can also be observed for variation of the load current as shown in Figure 2.14 and Figure 2.15 with source impedance.

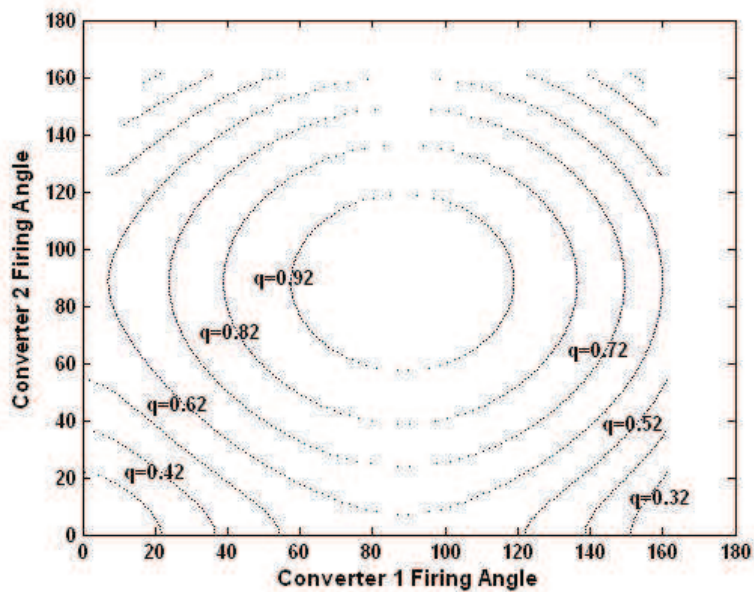


Figure 2.11: Range of firing angles for constant reactive power operation with source inductance

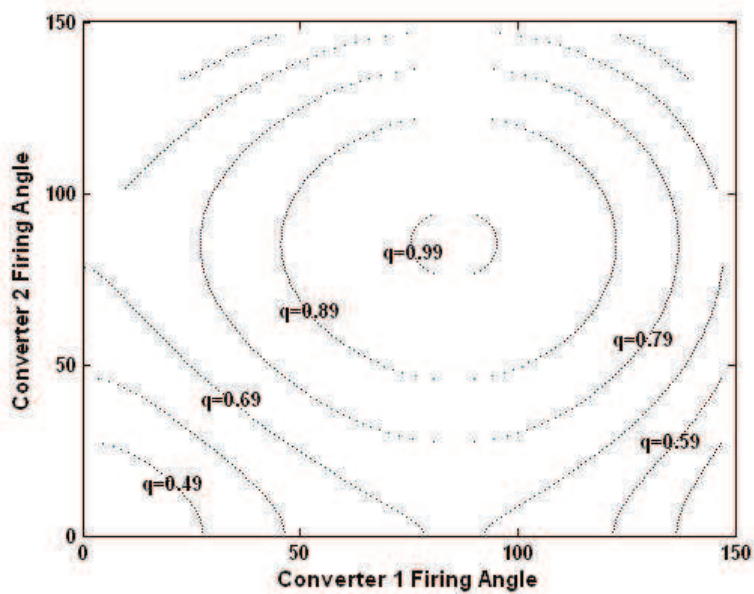


Figure 2.12: Range of firing angles for constant reactive power operation with source inductance

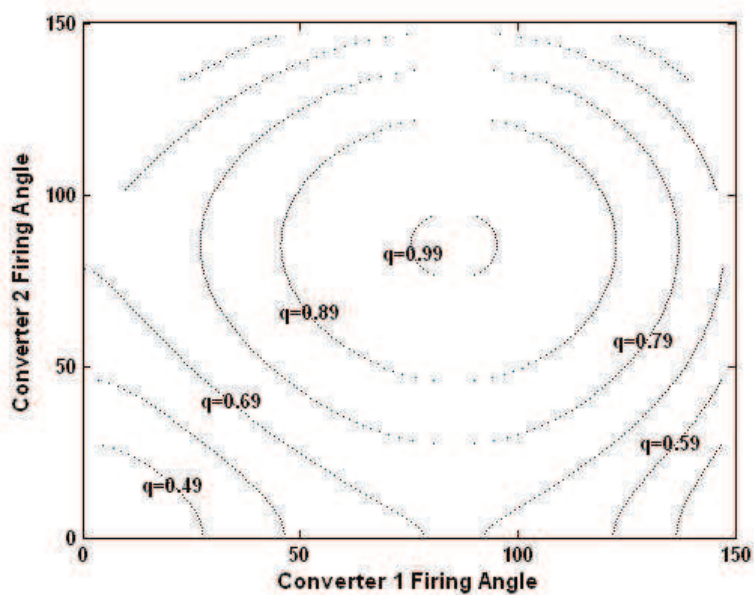


Figure 2.13: Range of firing angles for constant reactive power operation with source inductance effect.

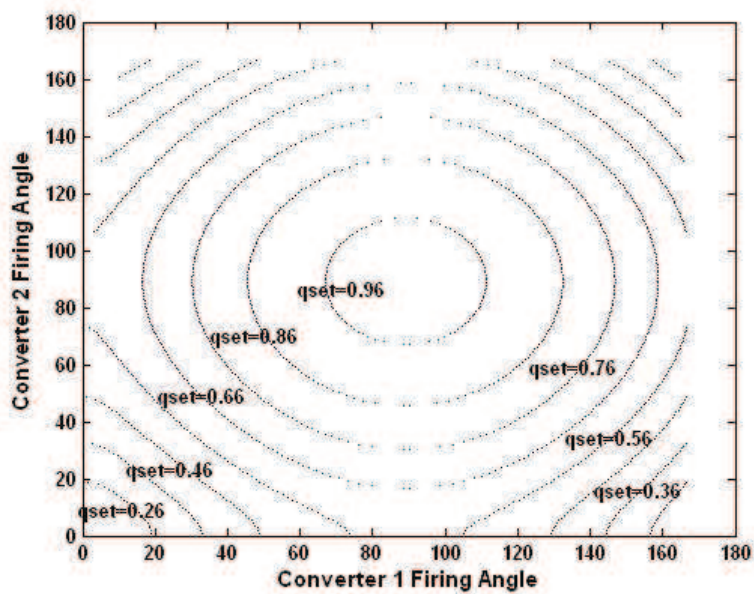


Figure 2.14: Range of firing angles for constant reactive power operation with variation in I_d

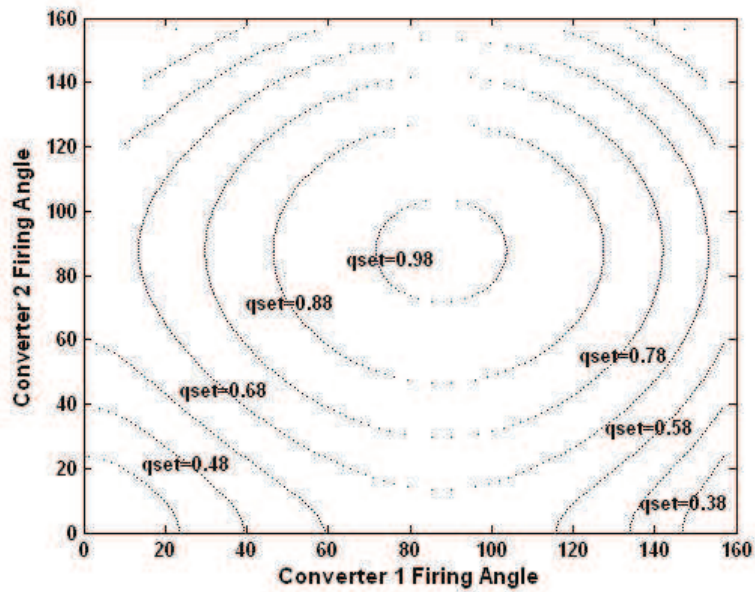


Figure 2.15: Range of firing angles for constant reactive power operation with variation in I_d

2.7 Constant active power operation

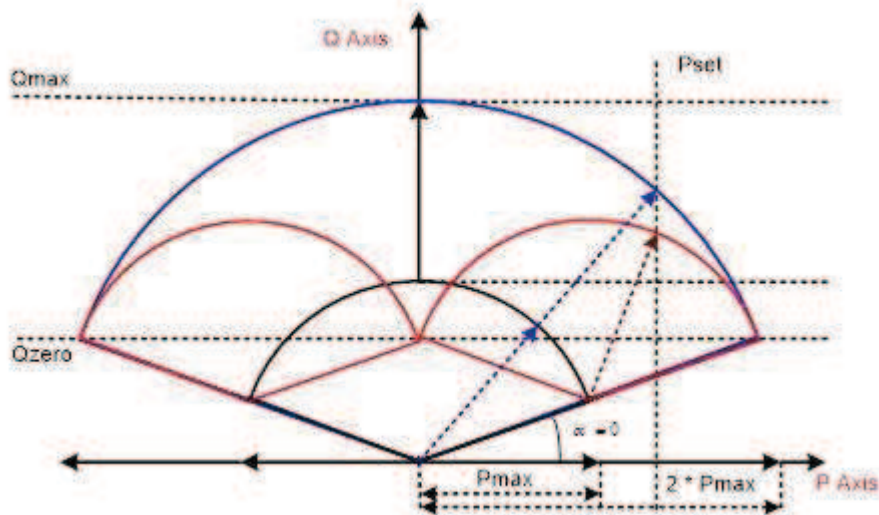


Figure 2.16: Limiting Firing angle operation of 12- pulse converter for P_{set} value

For a 12-pulse converter, the var drawn from the source for given active power demand will be maximum under symmetrical mode. Therefore for given active power demand,

only the minimum var condition has to be known. The 12-pulse converter operation in constant active power mode can be explained using Figure 2.16. In this case, when the converter is operated in asymmetrical mode, there will be a range of firing angles within which both the converters must operate to generate constant active power.

Under certain operating condition the desired net active power P_{set} can be expressed in per unit (p.u.) values as sum of the active power drawn by the each converter.

$$q_{set}(p.u.) = (\cos\phi_1 + \cos\phi_2) * 0.5 \quad (2.21)$$

Or

$$q_{set}(p.u.) = \frac{V_{do}I_d}{S_{max}}(\cos\phi_1 + \cos\phi_2) - \frac{2X_cI_d^2}{S_{max}} \quad (2.22)$$

at $\alpha_i = 0$

$$P_{max}(p.u.) = \left(1 - \frac{X_cI_d}{V_{do}}\right) \quad (2.23)$$

And

$$P_{min}(p.u.) = \left(\cos(\text{end} - \text{stop}) - \frac{X_cI_d}{V_{do}}\right) \quad (2.24)$$

So the P_{set} is varied between P_{min} and P_{max} . From Figure 2.9 it is observed that, when one of the converters is operated at $\alpha_1 = 0^\circ$, the other converter must operate at the firing angle

$$\alpha_2 = \cos^{-1} \left[2 \left(\frac{P_{set} + I_d^2 X_c}{S_{max}} \right) - \cos\alpha_1 \right] \quad (2.25)$$

Figure 2.17 shows the curves for the various combinations of the firing angles at the different values of P_{set} . At any value of active power transfer, the operating point of α_1, α_2 may lie at any point on the corresponding curve. The reactive power consumption depends on the positioning of α_1, α_2 on that curve. It is observed that the freedom of choice of α_1, α_2 reduces with the increase of active power transfer. As the source inductance is increased this range of is also smaller and end stop limit for the both converter is also decreasing. The value of the overlap angle is also depends on the load current. Figure 2.18 shows the variation the range of active power (p.u.) as the load current I_d is varied.

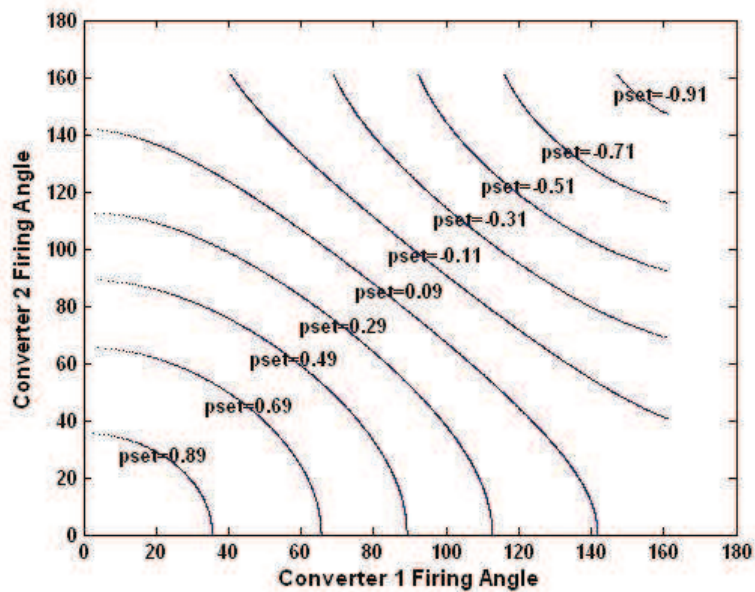


Figure 2.17: Range of firing angles for constant Active power

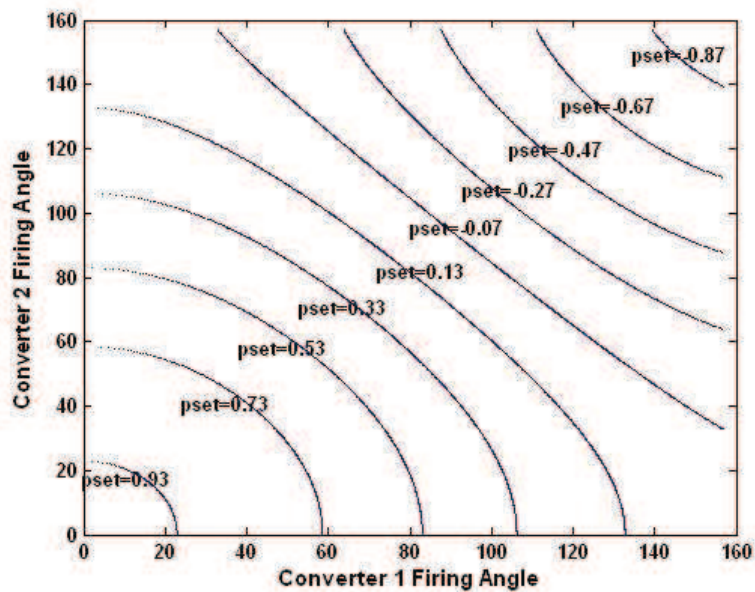


Figure 2.18: Range of firing angles for constant Active power

2.8 Active and Reactive Power for 12 pulse converter

Converter is simulated for equal and unequal firing angle mode. Active power drawn by converter is plotted by changing the firing angle of converter 2 by keeping converter 1 firing angle constant for different values. As converter 2 firing angle is increased, the power drawn by the 12 pulse converter is reduced as shown in Figure 2.19. Reactive power drawn by converter is also plotted for the same values of converter 2 firing angle by keeping converter 1 at constant value. The results are plotted in Figure 2.20.

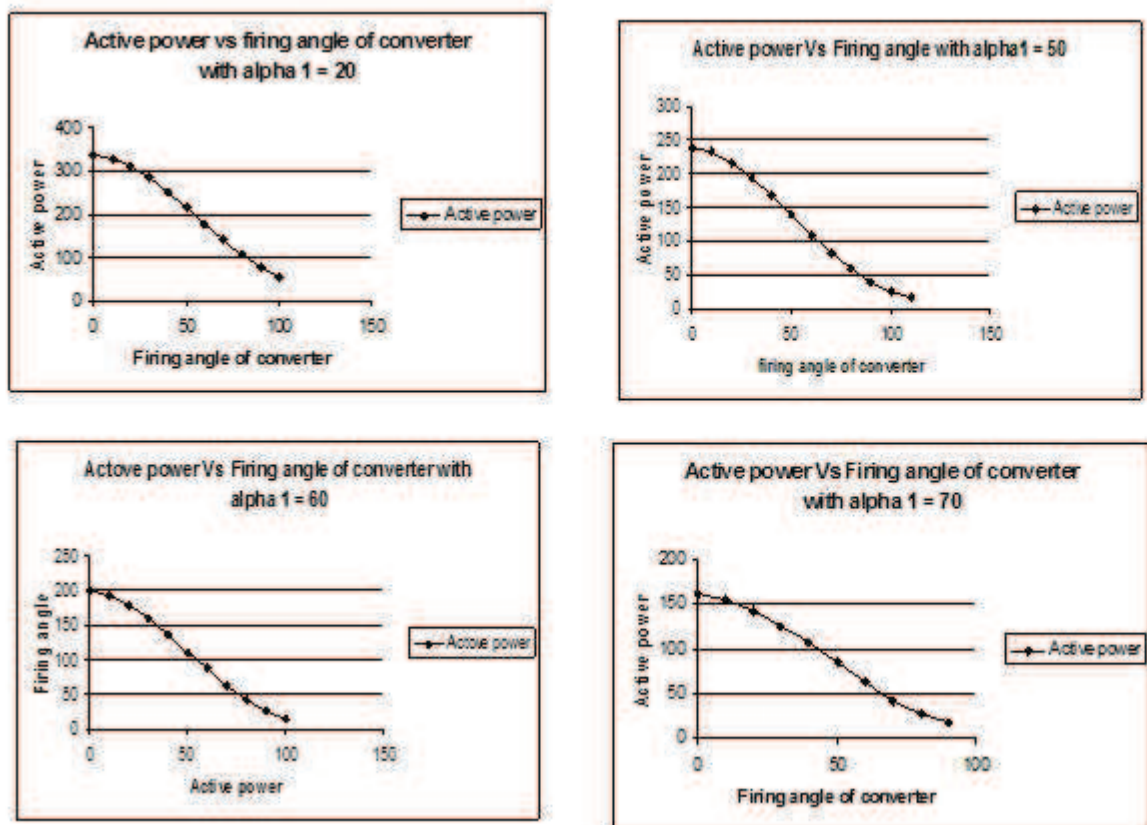


Figure 2.19: Active power Vs Converter 2 firing angle

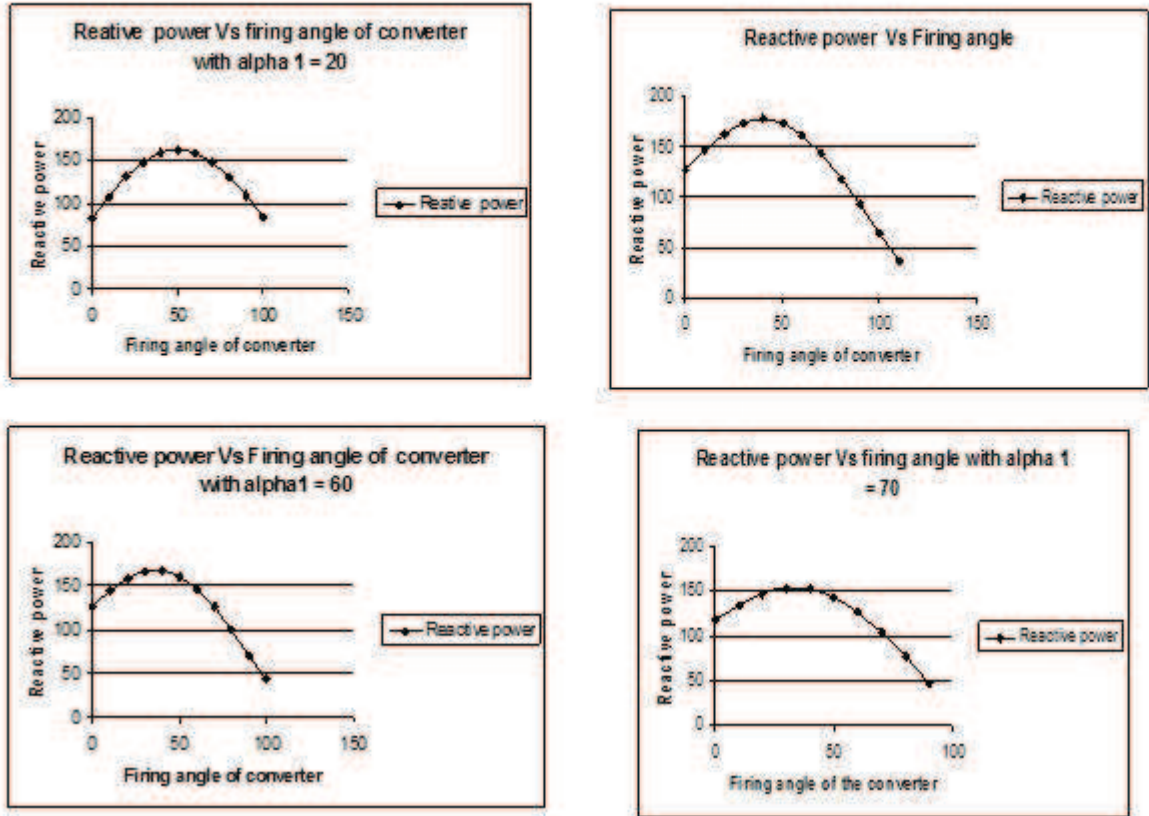


Figure 2.20: Reactive power Vs Converter 2 firing angle

2.9 Harmonics in 12-pulse converter

Because the thyristor conduction periods of each 3 pulse group are displaced in phase from those of all the other groups, a cancellation of certain harmonic components of current occur in those parts of the input ac circuit which carry the currents of more than one 3-pulse group. At the same time, those harmonic currents, which do not cancel, remain with the same relative amplitudes as in the 3-pulse converter. The following equation shows the input current expression in terms of Fourier expansion

$$F_1(\theta_i - \alpha) = \frac{1}{3} + \frac{\sqrt{3}}{\pi} [\sin(\theta_i - \alpha) - \frac{1}{2} \cos 2(\theta_i - \alpha)]$$

$$-\frac{1}{4}\cos 4(\theta_i - \alpha) - \frac{1}{5}\sin 5(\theta_i - \alpha) - \frac{1}{7}\sin 7(\theta_i - \alpha) + \frac{1}{8}\cos 8(\theta_i - \alpha) + \frac{1}{10}\cos 10(\theta_i - \alpha) + \frac{1}{11}\cos 11(\theta_i - \alpha) + \frac{1}{13}\cos 13(\theta_i - \alpha)\dots\dots] \quad (2.26)$$

2.9.1 Harmonic analysis of 6-pulse converter:

For a star connected primary of the input transformer, the supply current is given by

$$i_{SA} = F_1(\theta_i - \alpha) - F_1(\theta_i - \alpha + \pi)$$

$$i_{SA} = \frac{2\sqrt{3}}{\pi}[\sin(\theta_i - \alpha_1) - \frac{1}{5}\sin 5(\theta_i - \alpha_1) - \frac{1}{7}\sin 7(\theta_i - \alpha_1) + \frac{1}{11}\sin 11(\theta_i - \alpha_1) + \frac{1}{13}\sin 13(\theta_i - \alpha_1)\dots\dots] \quad (2.27)$$

Thus the amplitude of the fundamental component of waveform is $\frac{3}{\pi}$ * peak value and the harmonic components have the same frequencies and relative amplitudes as those of star connected input.

$$i_{SB} = 0.5F_1(\theta_i - \alpha + \frac{\pi}{6}) - 0.5F_1(\theta_i - \alpha - \frac{5\pi}{6}) + 0.5F_1(\theta_i - \alpha - \frac{\pi}{6}) - 0.5F_1(\theta_i - \alpha + \frac{5\pi}{6})$$

$$i_{SB} = \frac{3}{\pi}[\sin(\theta_i - \alpha_2) + \frac{1}{5}\sin 5(\theta_i - \alpha_2) + \frac{1}{7}\sin 7(\theta_i - \alpha_2) + \frac{1}{11}\sin 11(\theta_i - \alpha_2) + \frac{1}{13}\sin 13(\theta_i - \alpha_2)\dots\dots\dots]$$

2.9.2 Harmonic analysis of 12-pulse converter:

For obtaining a constant Var operation with wide-range of active power control, the 12-pulse converter has to be operated under asymmetrical mode. Under this mode $(6n \pm 1)$ input current harmonics for all integral values of n appear in the supply. Where as, in symmetrical mode, only $(6n \pm 1)$ current harmonics for all n= even integers are present. The general Fourier series expressions of $(6n \pm 1)$ harmonic components of the primary

input current in a 12-pulse converter can be expressed as follows:

For all odd value of n,

$$I_{6n\pm 1} = \frac{\sin((6n \pm 1)(\frac{\alpha_1 - \alpha_2}{2})) \cos((6n \pm 1)(wt - (\frac{\alpha_1 - \alpha_2}{2})))}{(6n \pm 1) * \cos(\frac{\alpha_1 - \alpha_2}{2}) \sin(wt - (\frac{\alpha_1 - \alpha_2}{2}))} \quad (2.28)$$

And, for all even value of n,

$$I_{6n\pm 1} = \frac{\cos((6n \pm 1)(\frac{\alpha_1 - \alpha_2}{2})) \cos((6n \pm 1)(wt - (\frac{\alpha_1 - \alpha_2}{2})))}{(6n \pm 1) * \cos(\frac{\alpha_1 - \alpha_2}{2}) \sin(wt - (\frac{\alpha_1 - \alpha_2}{2}))} \quad (2.29)$$

where,

α_1 = Firing angle of converter 1

α_2 = Firing angle of converter 2

The above expressions are ratio of harmonic magnitudes to the fundamental at those values of converter firing angles α_1 and α_2 .

Figure 2.21 presents the 3D plot of per unit $6n \pm 1$ harmonic magnitudes for $n=1,2$ of source current for simultaneous variation in firing angles of both the converters. It can also be observed from the figure that the maximum and minimum values of the p.u harmonics occur alternately at different combinations of α_1 and α_2 which can be obtained by the relationship expressed as follows:

For n =odd, the magnitude of the corresponding harmonic is zero when,

$$(6n \pm 1) * (\frac{\alpha_1 - \alpha_2}{2}) = \pi$$

And is maximum when,

$$(6n \pm 1) * (\frac{\alpha_1 - \alpha_2}{2}) = \frac{\pi}{2}$$

For n =even, the magnitude of the corresponding harmonic is zero when,

$$(6n \pm 1) * (\frac{\alpha_1 - \alpha_2}{2}) = \frac{\pi}{2}$$

And is maximum when,

$$(6n \pm 1) * \left(\frac{\alpha_1 - \alpha_2}{2}\right) = \pi$$

Using the expressions discussed above, in Figure 2.14(a), representing the 3-D plot of 5th harmonic input current, it can be observed that a minimum (zero) magnitude occurs at $(\alpha_1, \alpha_2) = (0,0), (0,72), (0,144), (72,0)$ and $(144,0)$ and a maximum occurs at $(\alpha_1, \alpha_2) = (0,36), (0,108), (0,180), (36,0), (108,0)$ and $(180,0)$. Similar arguments can be made for Figure 2.10 (b)-(d).

Input current of the 12-pulse converter for the six pulse bridges connected in series is give by

$$i_{12} = 0.464F_1(\theta_i - \alpha) - 0.464F_1(\theta_i - \alpha + \pi) + 0.268F_1(\theta_i - \alpha + \frac{\pi}{6})$$

$$-0.268F_1(\theta_i - \alpha + \frac{5\pi}{6}) - 0.268F_1(\theta_i - \alpha + \frac{\pi}{6}) - 0.268F_1(\theta_i - \alpha - \frac{5\pi}{6})$$

$$i_{12} = 1.024[\sin(\theta_i - \alpha) + \frac{1}{11}\sin 11(\theta_i - \alpha) + \frac{1}{13}\sin 13(\theta_i - \alpha).....] \quad (2.30)$$

Thus the amplitude of fundamental component is 1.024 X peak value. The harmonic components have frequencies of 11, 13 and in general X the fundamental frequency. Thus the amplitude of fundamental component is 1.024 X peak value. The harmonic components have frequencies of 11, 13 and in general $(12n \pm 1)$ X the fundamental frequency.

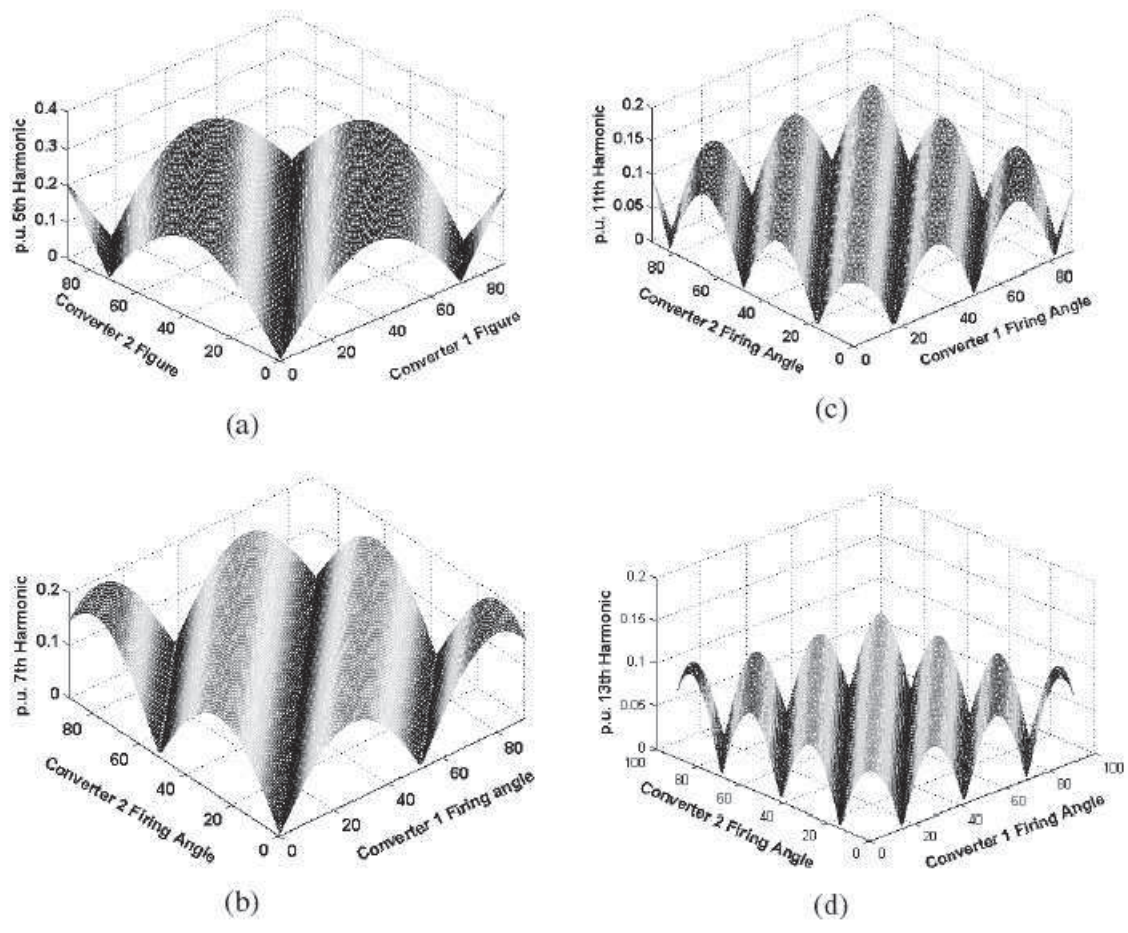


Figure 2.21: per unit 5^{th} , 7^{th} , 11^{th} and 13^{th} harmonics for simultaneous variation of converter 1 and 2 firing angles

2.10 Harmonic analysis of the 12-pulse converter operating under unequal firing angle

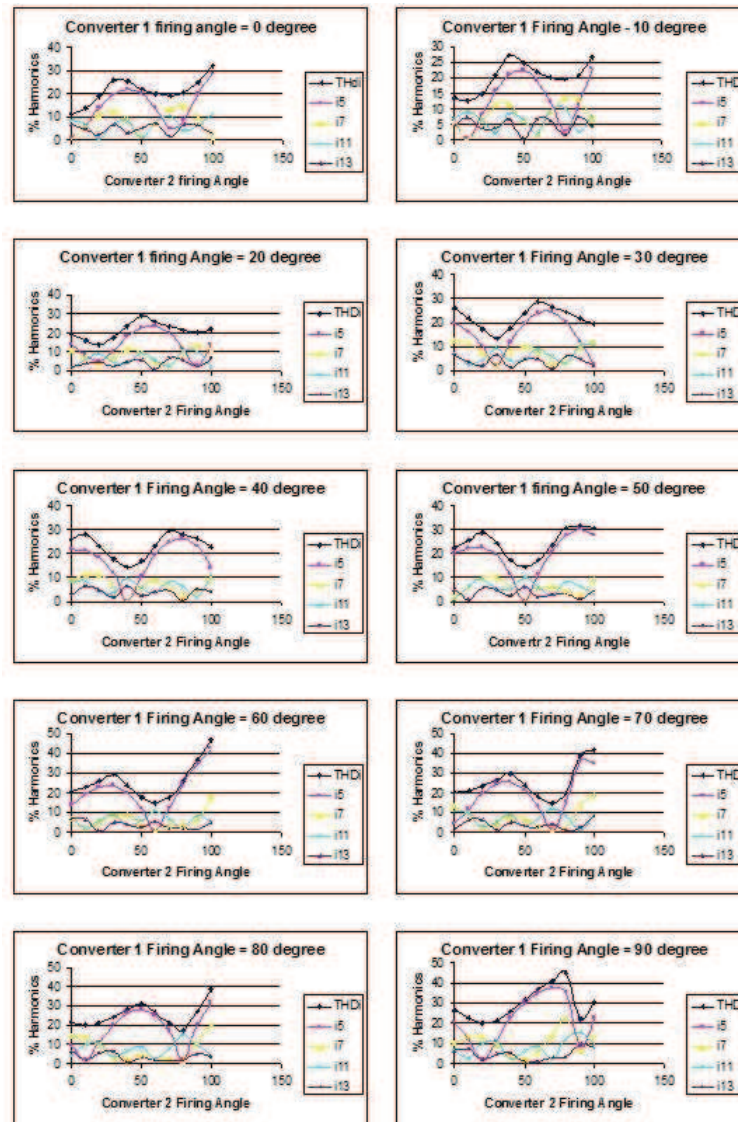


Figure 2.22: % THD 5th, 7th, 11th and 13th harmonic component Vs Converter 2 firing angle

12 pulse converter is simulated for equal and unequal mode of operation. The % Total Harmonic Distortion (THD) is measured along with 5th, 7th, 11th and 13th order harmonic current component for different values of converter 2 firing angle while keeping converter 1 firing angle constant for different values. As shown in Figure 2.22, it follows $(6n \pm 1)$

for equal firing angle and $(12n \pm 1)$ for unequal firing angle mode. The total patterns are added for % THD and plotted as shown in Figure 2.23 where variation of % THD is observed. Figure 2.24 and Figure 2.25 shows the variation of supply voltage, current drawn by the converter for different values for equal and unequal firing angle mode.

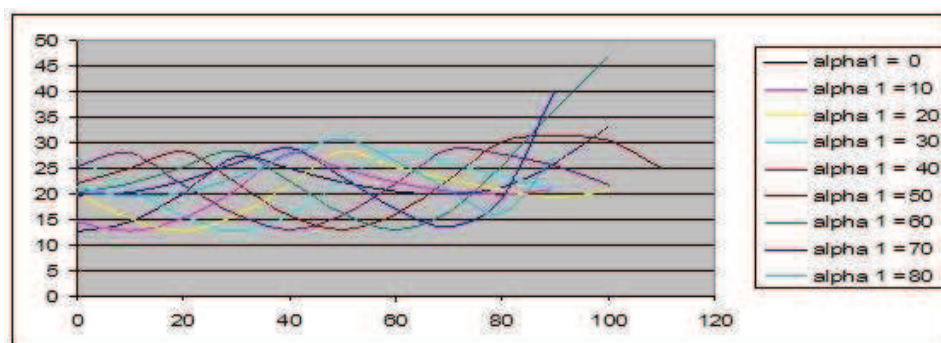


Figure 2.23: waveform for equal firing angle

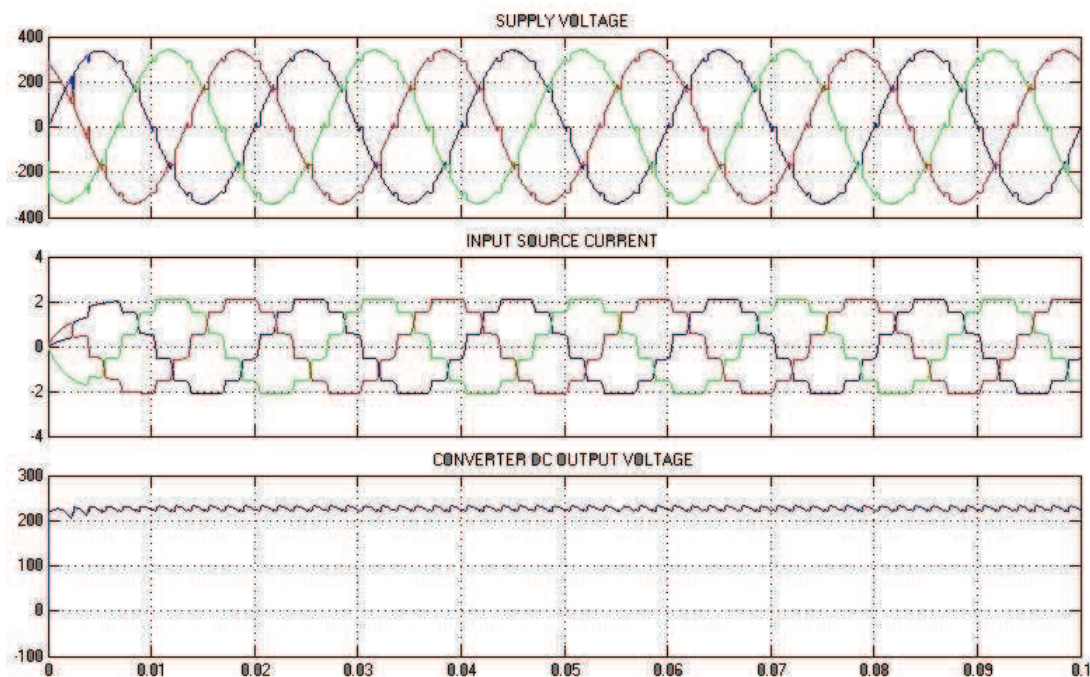


Figure 2.24: waveform for equal firing angle

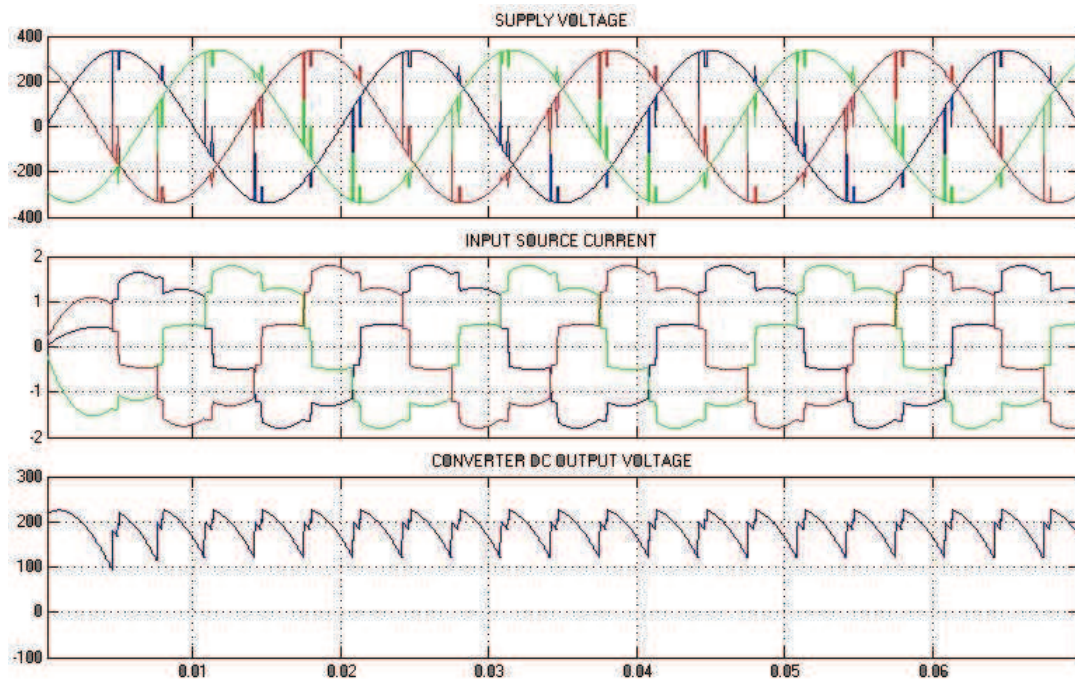


Figure 2.25: waveform for unequal firing angle

2.11 Conclusion

The performance of the 12-pulse converter under for the constant reactive power and the constant active power has been investigated. The variation of the active power and reactive power under equal and unequal firing angle has been calculated. For equal firing angle, the harmonic profile of the converter is found to be $(12n \pm 1)$. Because of the unequal firing angle, the harmonic profile of the converter is found to be $(6n \pm 1)$. The variation of magnitude of lower order harmonics like 5^{th} , 7^{th} , 11^{th} and 13^{th} with variation of converters firing angle is carried out.